2011 American Control Conference
on O'Farrell Street, San Francisco, CA, USA
June 29 - July 01, 2011

Adaptive Decoupling Control of the Forced-Circulation Evaporation System Using Neural Networks and Multiple Models

Yonggang Wang, Tianyou Chai, Jun Fu, and Jing Sun

Abstract—**Control objectives of the forced-circulation evaporation process of alumina production include maintaining the liquid level and fast tracking of the product density to its setpoint. Due to the strong coupling between the level control and product density control loops and high nonlinearities in the process, conventional control strategies can not achieve satisfactory control performance and meet production demands. Viewing the forced-circulation evaporation system and valves as a generalized plant, a nonlinear multi-model adaptive decoupling control strategy is proposed. The nonlinear adaptive decoupling controller includes a linear adaptive decoupling controller, a neural-network-based nonlinear adaptive decoupling controller, and a switching mechanism. The linear adaptive decoupling controller is used to reduce the coupling between the two loops. The neural-network-based nonlinear adaptive decoupling controller is employed to improve the transient performance and mitigate effects of the nonlinearities on the system, and the switching mechanism is introduced to guarantee the input-output stability of the closed-loop system. Simulation results show that the proposed method can decouple the loops effectively for the forced-circulation evaporation system and can improve the evaporation efficiency.**

I. Introduction

FORCED-circulation evaporation system is the last stage of the liquor burning process in the evaporation system associated with Bayer process for alumina production in an alumina refinery. The objective of the operation is to remove the organic impurities of the spent caustic liquor so that the liquor can be recycled. In order to improve the evaporation efficiency and to keep operation smooth, the liquid level of the evaporator should avoid large fluctuations. The product density set point must also be tracked quickly.

Level control and product density control of the forced-circulation system are challenging problems because of their unique characteristics such as complex dynamics, high nonlinearity and strong coupling between the dual loops [1]. Therefore, good performance for the forced circulation evaporation system is difficult to achieve using a conventional decentralized control system [2]. In order to reduce the coupling, several effective methods were proposed in the literature [3-7]. However, those designs did not take into account the dynamic characteristics of the control valves. Thus the dynamics of the sub-systems and information can not be effectively used to improve overall dynamic performances of the system. Moreover, parametric uncertainties of the evaporation process were not considered in the afore-mentioned literatures.

Over last decades, effectiveness of adaptive decoupling control technology has been demonstrated in solving the parameter uncertainties problems and in reducing the coupling among multiple control loops [8-10]. However, because of the strong nonlinearities in the forced-circulation evaporation system, the adaptive decoupling technology sometimes cannot achieve desired performances. The integration of adaptive control and neural networks has made significant progress in recent years [11-15]. However, its applications to complex systems such as the forced-circulation evaporation system have not been demonstrated.

This paper views the actuating valves and the forced-circulation evaporation system as a generalized plant. To decouple the level control loop from the product density control loop of the forced- circulation system, an adaptive nonlinear decoupling controller using neural network and multiple models is proposed. The design consists of three elements: the linear adaptive decoupling controller used to reduce strong coupling between the two loops, the neural-network-based nonlinear adaptive controller employed to improve the transient performance and mitigate nonlinearities effects, and the switching mechanism introduced to guarantee the input-output stability of the closed-loop system. Simulation results show that the proposed method can effectively decouple the two loops for the forced-circulation evaporation system and can improve the evaporation efficiency.

The rest of the paper is organized as follows. Forced-circulation evaporation system is described in Section II. The generalized plant model of the forced-circulation evaporation system is developed in Section III. The nonlinear

This work was supported by the State Key Program of National Natural Science of China Grant (60534010), the National Natural Science Foundation of China (61020106003,61004009), the 111 project (B08015), the Funds for Creative Research Groups of China Grant (60521003), the Program for New Century Excellent Talents in University (NCET-05-0294) in China, the Fundamental Research Funds for the Central Universities (N100708001, N100408004) and the Specialized Research Fund for the Doctoral Program of Higher Education of China under Grant 20100042120033.

Y.G. Wang, T.Y. Chai (corresponding author), J. Fu are State Key Laboratory of Integrated Automation for Process Industry (Northeastern University) and Research Center of Automation, Northeastern University, Shenyang 110004, China (e-mail: wygvern@gmail.com).

J. Sun is with the Department of Naval Architecture and Marine Engineering at the University of Michigan, Ann Arbor, MI 48109, U.S.A., Email: jingsun@umich.edu.

adaptive multi-model control strategy is proposed in Section IV. In Section V, simulation results are presented to illustrate the effectiveness of the proposed method. Section VI concludes this paper.

II. Forced-circulation Evaporation System Description

The schematic diagram of the forced-circulation evaporation system is shown in Fig.1. The system is mainly composed of flash tank, pump and steam heaters.

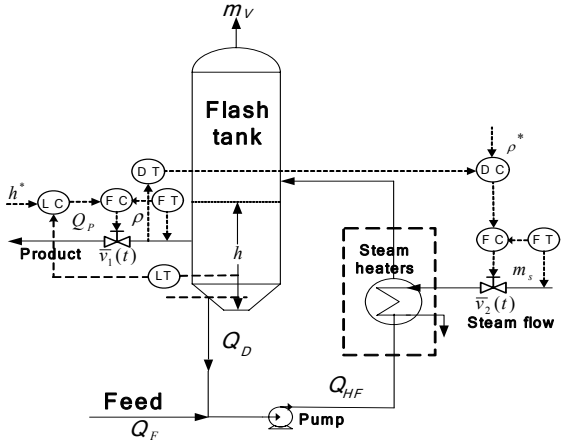

Fig.1 Schematic of the forced-circulation evaporation system

The feed (Q_F) is mixed with a high volumetric flow rate of recycling liquor (Q_D) and is pumped into a heat exchanger which is heated by the steam. The liquid passes to the flash tank where the liquid and the vapor are separated. The liquid is recycled with some drowned off as product. The vapor (m_V) is usually used as heating steam for other processes.

The current control strategy of the forced-circulation system is accomplished by using muti-loop cascade SISO controller. The flow rate of the heat steam (m_s) is manipulated to control the product density (ρ), while the valve ($\bar{v}_2(t)$) opening is adjusted for the heat steam (m_s). The flash tank liquid level (h) is controlled by the discharge liquor flow (Q_P), while the valve ($\bar{v}_1(t)$) opening is adjusted for the discharge liquor flow (Q_P). The conventional cascade control strategy is difficult to achieve satisfactory control performance mainly for the following reasons. First, the dual cascade loops have strong interactions and there are many disturbances such as feed flow (Q_F) and feed density (ρ_f) in the forced-circulation system. Second, the parameters of specific heat of the liquor change with the different feed flow, which leads to changes of dynamic characteristics of the forced-circulation system.

III. Generalized Plant of the Forced-circulation System

A. Dynamic modeling

The dynamic model of the forced-circulation system can be derived from mass and energy balances [2]. The model equations are given below.

1) Flash tank level:

$$\frac{dh}{dt} = \frac{1}{A}(Q_F - Q_P - \frac{m_V}{\rho_w}) \tag{1}$$

2) Flash tank liquid product density

$$\frac{d\rho}{dt} = \frac{1}{Ah}(Q_F\rho_F(\frac{\rho}{\rho_F} - 1) - m_V(\frac{\rho}{\rho_w} - 1)) \tag{2}$$

3) Flash tank liquid discharge temperature

$$\frac{dT}{dt} = \frac{1}{cAh\rho}[Q_{HF}\rho_{HF}c_{HF}T_{HF} + \lambda_S m_s - m_V\lambda_v - (Q_{HF}\rho_{HF} - m_V)cT] \tag{3}$$

where

$$m_V = \frac{Q_F\rho_F c_F T_F - cQ_P\rho T + m_s\lambda_S}{\lambda_V} \tag{4}$$

$$T_{HF} = \frac{Q_F\rho_F c_F T_F + Q_D cT\rho}{Q_{HF}\rho_{HF}c_{HF}} \tag{5}$$

$$Q_{HF}\rho_{HF} = Q_D\rho + Q_F\rho_F \tag{6}$$

The detailed description of the model can be found in [2].

B. Generalized plant

Substituting (4)-(6) into (1)-(3) yields the following dynamic model for the forced-circulation system:

$$\frac{dh}{dt} = \frac{1}{A\rho_w\lambda_V}[Q_F(\rho_w\lambda_V - \rho_F c_F T_F) - \rho_w\lambda_V Q_P + cT\rho Q_P - \lambda_S m_s] \tag{7}$$

$$\frac{d\rho}{dt} = \frac{1}{A\lambda_V\rho_w h}[Q_F\lambda_V\rho_w\rho - Q_F\lambda_V\rho_w\rho_F - (Q_F\rho_F c_F T_F - cT\rho Q_P + \lambda_s m_s)(\rho - \rho_w)] \tag{8}$$

$$\frac{dT}{dt} = \frac{1}{A\lambda_V h\rho}[Q_F\rho_F(c_F T_F - \lambda_V)T + (\lambda_V - cT)\rho TQ_P + \lambda_s T m_s] \tag{9}$$

The above model does not consider of dynamic characteristic of the control valves. From a control engineering point of view, the generalized plant of the evaporation system corresponds to a classical cascade feedback control system. The inner loops correspond to the fast dynamics which is associated to the actuators, and the outer loop corresponds to the control of the evaporation system which is described by a nonlinear dynamic model. The generalized plant integrates the subsystem and the evaporation system information.

In order to obtain the generalized plant of the forced-circulation system, the control valves model should be derived. The valve dynamic model can be acquired using the experimental data.

Model of the discharge flow (where $\bar{v}_1$ and q_1 are input variable and output variable, respectively) can be presented as follows:

$$\bar{v}_1(s) / q_1(s) = 1.74 / (5.28s + 1) \tag{10}$$

Model of the steam flow (where $\bar{v}_2$ and q_2 are input variable and output variable, respectively) can be presented as follows:

$$\bar{v}_2(s) / q_2(s) = 0.3 / (4.68s + 1) \tag{11}$$

According to the above dynamic models, the PID controller parameters can be acquired as follows:

$Kp1$=0.9976; $Ki1$=0.1903; $Kd1$=0; $Kp2$=4.9131; $Ki2$=1.1789; $Kd2$=0. Substituting the controller into the dynamic model, we can acquire the close-loop equation as follows:

$$q_1(s)/u_1(s) = (0.3288s + 1.7276)/(s^2 + 0.5181s + 1.7276) \quad (12)$$

$$q_2(s)/u_2(s) = (0.3149s + 0.2671)/(s^2 + 0.5286s + 0.2671) \quad (13)$$

where q_1 and q_2 are discharge flow and the steam flow, respectively; u_1 and u_2 are discharge flow setpoint and steam flow setpoint, respectively.

Define $h = x_1, \rho = x_2$ and $T = x_3$. We can transform the (12) and (13) into the following state space form:

$$\begin{bmatrix} \dot{x}_4 \\ \dot{x}_5 \end{bmatrix} = \begin{bmatrix} 0 & 1 \\ -1.7276 & -0.5181 \end{bmatrix} \begin{bmatrix} x_4 \\ x_5 \end{bmatrix} + \begin{bmatrix} 0 \\ 1 \end{bmatrix} u_1 \quad (14)$$

$$q_1 = \begin{bmatrix} 1.7276 & 0.3288 \end{bmatrix} \begin{bmatrix} x_4 \\ x_5 \end{bmatrix} \quad (15)$$

$$\begin{bmatrix} \dot{x}_6 \\ \dot{x}_7 \end{bmatrix} = \begin{bmatrix} 0 & 1 \\ -0.2671 & -0.5288 \end{bmatrix} \begin{bmatrix} x_6 \\ x_7 \end{bmatrix} + \begin{bmatrix} 0 \\ 1 \end{bmatrix} u_2 \quad (16)$$

$$q_2 = \begin{bmatrix} 0.2671 & 0.3149 \end{bmatrix} \begin{bmatrix} x_6 \\ x_7 \end{bmatrix} \quad (17)$$

Substituting (15)- (17) into (7)- (9) and combining the result with (14)- (16), we can derive the generalized plant as follows:

$$\begin{cases} \dot{x}_1 = \dfrac{1}{A\rho_w\lambda_V}[Q_F(\rho_w\lambda_V - \rho_F c_F T_F) - (\rho_w\lambda_V - cx_2x_3) \\ \quad (1.7276x_4 + 0.3288x_5) - \lambda_S(0.2671x_6 + 0.3149x_7)] \\ \dot{x}_2 = \dfrac{1}{A\lambda_V\rho_w x_1}[Q_F\lambda_V\rho_w x_2 - Q_F\lambda_V\rho_w\rho_F - (Q_F\rho_F c_F T_F - cx_2x_3 \\ \quad (1.7276x_4 + 0.3288x_5) + \lambda_s(0.2671x_6 + 0.3149x_7))(x_2 - \rho_w)] \\ \dot{x}_3 = \dfrac{1}{A\lambda_V x_1 x_2}[Q_F\rho_F(c_F T_F - \lambda_V)x_3 + (\lambda_V - cx_3)x_2x_3 \\ \quad (1.7276x_4 + 0.3288x_5) + \lambda_s x_3(0.2671x_6 + 0.3149x_7)] \\ \dot{x}_4 = x_5 \\ \dot{x}_5 = -1.7276x_4 - 0.5181x_5 + u_1 \\ \dot{x}_6 = x_7 \\ \dot{x}_7 = -0.2671x_6 - 0.5288x_7 + u_2 \end{cases} \quad (18)$$

Eq. (18) can be written as

$$\dot{x} = f(x_1, x_2, x_3, x_4, x_5, x_6, x_7) + Bu(t) \quad (19)$$

where $u(t) = [u_1(t) \quad u_2(t)]^T$; $B = \begin{bmatrix} 0 & 0 & 0 & 0 & 1 & 0 & 0 \\ 0 & 0 & 0 & 0 & 0 & 0 & 1 \end{bmatrix}^T$; and

$$x(t) = [x_1(t) \quad x_2(t) \quad x_3(t) \quad x_4(t) \quad x_5(t) \quad x_6(t) \quad x_7(t)]^T$$

Define system outputs: $y(t) = Cx(t)$ (20)

where $C = \begin{bmatrix} 1 & 0 & 0 & 0 & 0 & 0 & 0 \\ 0 & 1 & 0 & 0 & 0 & 0 & 0 \end{bmatrix}$, $y(t) = [y_1(t) \quad y_2(t)]^T$

Discrete model of the generalized plant can be obtained via the Euler method by selecting the sampling period T and can be transformed into the NARMA as follows:

$$y_1(k+1) = f_{y1}(y_1(k), y_1(k-1), y_2(k), y_2(k-1), u_1(k), u_1(k-1), u_2(k), u_2(k-1)) \quad (21)$$

$$y_2(k+1) = f_{y2}(y_1(k), y_1(k-1), y_2(k), y_2(k-1), u_1(k), u_1(k-1), u_2(k), u_2(k-1)) \quad (22)$$

Eq. (21) and Eq. (22) can be rewritten as a general form:

$$y(k) = f[y(k-1), \cdots, y(k-n_a), u(k-1), \cdots, u(k-n_b-1)] \quad (23)$$

where $u(k) = [u_1(k) \quad u_2(k)]^T \in \mathbf{R}^2$ denotes the discharge flow setpoint and steam flow setpoint. $y(k) = [y_1(k) \quad y_2(k)]^T \in \mathbf{R}^2$ denotes the system outputs. $f[\cdot] \in R^2$ is a smooth vector-valued nonlinear function; n_a and n_b are the system orders.

IV. Nonlinear Adaptive Multi-Model Control Strategy

In this Section, the generalized plant is first reformulated to be suitable for controller design. The generalized plant of the forced-circulation system can be decomposed into a linear model incorporating a nonlinear term around the operating point, as expressed in the following formulation [15]:

$$\begin{bmatrix} y_1(k) \\ y_2(k) \end{bmatrix} = -\begin{bmatrix} a_{11}(z^{-1}) & 0 \\ 0 & a_{22}(z^{-1}) \end{bmatrix} \begin{bmatrix} y_1(k-1) \\ y_2(k-1) \end{bmatrix} + \begin{bmatrix} b_{11}(z^{-1}) & b_{12}(z^{-1}) \\ b_{21}(z^{-1}) & b_{22}(z^{-1}) \end{bmatrix} \begin{bmatrix} u_1(k-1) \\ u_2(k-1) \end{bmatrix} + \begin{bmatrix} v_1(k-1) \\ v_2(k-1) \end{bmatrix} \quad (24)$$

where $a_{ii}(z^{-1})$ and $b_{ij}(z^{-1})$ are polynomials of z^{-1}. $v(k-1) = v[y(k-1), \cdots, y(k-n_a), u(k-1), \cdots, u(k-n_b-1)] \in R^2$ is the higher order nonlinear item.

Eq. (24) can be rewritten as follows:

$$A(z^{-1})y(k) = \bar{B}(z^{-1})u(k-1) + \bar{\bar{B}}(z^{-1})u(k-1) + v(k-1) \quad (25)$$

where

$$A(z^{-1}) = \begin{bmatrix} 1 + z^{-1}a_{11}(z^{-1}) & 0 \\ 0 & 1 + z^{-1}a_{22}(z^{-1}) \end{bmatrix};$$

$$\bar{B}(z^{-1}) = \begin{bmatrix} b_{11}(z^{-1}) & 0 \\ 0 & b_{22}(z^{-1}) \end{bmatrix}; \quad \bar{\bar{B}}(z^{-1}) = \begin{bmatrix} 0 & b_{12}(z^{-1}) \\ b_{21}(z^{-1}) & 0 \end{bmatrix}.$$

Remark: Considering the physical restrictions of the forced-circulation, the nonlinear term $v(k-1)$ is assumed to be bounded in this paper.

A. Nonlinear Decoupling Controller

We can construct nonlinear decoupling controller which makes the system outputs $y(k)$ track the reference value $w(t)$ in the following formulation:

$$\bar{H}(z^{-1})u(k) = K_I w(k) - L(z^{-1})y(k) - \bar{\bar{H}}(z^{-1})u(k-1) - \bar{K}(z^{-1})v(k) \quad (26)$$

where $\bar{H}(z^{-1})$, $L(z^{-1})$ and K_I, are diagonal polynomial matrix and diagonal constant matrix, respectively. The decoupling compensator $\bar{\bar{H}}(z^{-1})$, which is a polynomial matrix with zero diagonal elements, is designed to decouple control loops. The nonlinear compensator $\bar{K}(z^{-1})$, which is a diagonal polynomial matrix, is employed to eliminate the influence of the nonlinear item $v(k-1)$ on the closed-loop system.

As can be seen from (26), the linear decoupling controller can be written as:

$$\bar{H}(z^{-1})u(k) = K_I w(k) - L(z^{-1})y(k) - \bar{\bar{H}}(z^{-1})u(k-1) \quad (27)$$

Substituting (26) into (25) yields:

$$\begin{aligned}&[\bar{H}A(z^{-1}) + z^{-1}L\bar{B}(z^{-1})]y(k+1) = \bar{B}(z^{-1})K_I w(k) + \\ &[\bar{H}\bar{\bar{B}}(z^{-1}) - z^{-1}\bar{B}\bar{\bar{H}}(z^{-1})]u(k) + [\bar{H}(z^{-1}) - \bar{B}\bar{K}(z^{-1})]v(k)\end{aligned} \quad (28)$$

Thus, from (28), the coupling effect and the tracking errors can be eliminated in the steady state of the closed-loop system, provide that the matrices $\bar{\bar{H}}(z^{-1})$ and $\bar{K}(z^{-1})$ satisfy the following equations:

$$[\bar{H}(1)A(1) + L(1)\bar{B}(1)] = \bar{B}(1)K_I \quad (29)$$

$$\bar{H}(1)\bar{\bar{B}}(1) = \bar{B}(1)\bar{\bar{H}}(1) \quad (30)$$

$$\bar{H}(1) = \bar{B}(1)\bar{K}(1) \quad (31)$$

B. Parameters Selection

To choose matrices K_I, $\bar{\bar{H}}(z^{-1})$, $L(z^{-1})$ and $\bar{K}(z^{-1})$ in (26), the following performance index is introduced based on generalized predictive control law:

$$\begin{aligned}J = \sum_{j=1}^{N} \| & y(k+j) - r_j w(k+j) + S_j(z^{-1})u(k+j-1) + \\ & K_j(z^{-1})v(k+j-1)\|^2_{\lambda_j} + \sum_{j=1}^{N} \left\|u(k+j-1)\right\|^2_{Q_j(z^{-1})}\end{aligned} \quad (32)$$

where N denotes a prediction range, r_j, λ_j are diagonal weighting matrices; $K_j(z^{-1})$ is a diagonal polynomial matrix about z^{-1}; $S_j(z^{-1})$ is a polynomial matrix with zero diagonal elements that can eliminate coupling; $Q_j(z^{-1})$ are diagonal weighting matrices as expressed in the following formulation:

$$\begin{aligned}&Q_1(z^{-1}) = diag[q_0^{11} + q_1^1 z^{-1} + ...q_{m_1}^1 z^{-m_1} \quad q_0^{12} + q_1^2 z^{-1} + ...q_{m_2}^2 z^{-m_2}]_{2\times 2} = \\ &diag[q_0^{11} + z^{-1}Q_{11}(z^{-1}) \quad q_0^{12} + z^{-1}Q_{12}(z^{-1})]_{2\times 2} \\ &Q_j(z^{-1}) = diag[q_0^{j1} \quad q_0^{j2}]_{2\times 2} \qquad j = 2,3,.....N\end{aligned}$$

where $Q_1(z^{-1})$ is a diagonal polynomial matrix about z^{-1}, $Q_j(z^{-1}), j = 1...N$ are diagonal constant matrices. In order to obtain *j*-step ahead predictor, we introduce the following Diophantine equations:

$$I = E_j(z^{-1})A(z^{-1}) + z^{-j}F_j(z^{-1}) \quad (33)$$

$$E_j(z^{-1})\bar{B}(z^{-1}) = G_j(z^{-1}) + z^{-j}H_j(z^{-1}) \quad (34)$$

$$E_j(z^{-1})\bar{\bar{B}}(z^{-1}) = \bar{\bar{G}}_j(z^{-1}) + z^{-j}\bar{\bar{H}}_j(z^{-1}) \quad (35)$$

where $E_j(z^{-1}), F_j(z^{-1}), G_j(z^{-1}), H_j(z^{-1})$ are diagonal polynomial matrices about z^{-1}; $\bar{\bar{G}}_j(z^{-1}), \bar{\bar{H}}_j(z^{-1})$ are polynomial matrices with zero diagonal elements as expressed in the following formulation:

$$\begin{aligned}&E_j(z^{-1}) = \sum_{i=0}^{j-1} E_i z^{-i}, F_j(z^{-1}) = \sum_{i=0}^{n_a-1} F_i z^{-i}, G_j(z^{-1}) = \sum_{i=0}^{j-1} G_i z^{-i}, \\ &H_j(z^{-1}) = \sum_{i=0}^{n_b-1} H_i z^{-i}, \bar{\bar{G}}_j(z^{-1}) = \sum_{i=0}^{j-1} \bar{\bar{G}}_i z^{-i}, \bar{\bar{H}}_j(z^{-1}) = \sum_{i=0}^{n_b-1} \bar{\bar{H}}_i z^{-i},\end{aligned}$$

With (25), (33)-(35), *j*-step ahead predictor can be given by:

$$\begin{aligned}y(k+j) = {} & F_j(z^{-1})y(k) + G_j(z^{-1})u(k+j-1) + H_j(z^{-1})u(k-1) + \\ & \bar{\bar{G}}_j(z^{-1})u(k+j-1) + \bar{\bar{H}}_j(z^{-1})u(k-1) + E_j(z^{-1})v(k+j-1)\end{aligned} \quad (36)$$

Choose $S_j(z^{-1})$:

$$S_j(z^{-1})u(k+j-1) + \bar{\bar{G}}_j(z^{-1})u(k+j-1) + \bar{\bar{H}}_j(z^{-1})u(k-1) = \bar{\bar{M}}_j(z^{-1})u(k-1) \quad (37)$$

where $\bar{\bar{M}}_j(z^{-1})$ are polynomial matrices with zero diagonal elements. Substituting $y(k+j)$ into the performance (32) index yields:

$$\begin{aligned}J = \sum_{j=1}^{N} \| & F_j(z^{-1})y(k) + G_j(z^{-1})u(k+j-1) + H_j(z^{-1})u(k-1) + \\ & \bar{\bar{M}}_j(z^{-1})u(k-1) - r_j w(k+j) + [E_j(z^{-1}) + K_j(z^{-1})] \\ & v(k+j-1)\|^2_{\lambda_j} + \sum_{j=1}^{N} \left\|u(k+j-1)\right\|^2_{Q_j(z^{-1})}\end{aligned} \quad (38)$$

Minimizing the cost function J with respect to U leads to:

$$\begin{aligned}U = {} & (G^T\lambda G + Q_0)^{-1}\{G^T\lambda[RW - Fy(k) - Hu(k-1) \\ & - \bar{\bar{M}}u(k-1) - (E+K)V] - \sum_{i=1}^{m} Q_i z^{-i} U\}\end{aligned} \quad (39)$$

where $Q_0 = diag[q_0^{11}, q_0^{12}, q_0^{21}, q_0^{22}.....q_0^{N1}, q_0^{N2}]$, and $Q_i = \text{diag}[q_i^1,...,q_i^2,0,...0], i = 1....m, m = \max[m_1\ m_2]$, G is lower triangular Toeplitz matrix which are the coefficients of $G_j(z^{-1})$. Let $P = [P_1, P_2, ...P_N]$ be the first 2 rows of $(G^T\lambda G + Q_0)^{-1}G^T\lambda$, and $P' = [P_1', P_2', ...P_N',]$ be the first 2 rows of $(G^T\lambda G + Q_0)^{-1}$, where $P_i\ (i = 1,\cdots,N)$ and $P_i'\ (i = 1,\cdots,N)$ are 2×2 diagonal matrixes. Then:

$$\begin{aligned}u(k) = {} & P \times [RW - Fy(k) - Hu(k-1) - \bar{\bar{M}}u(k-1) \\ & - (E+K)V] - P_1'Q_1'(z^{-1})u(k-1)\end{aligned} \quad (40)$$

where $Q_1'(z^{-1}) = diag[Q_{11}(z^{-1}) \quad Q_{12}(z^{-1})]_{2\times 2}$. We define

$$R_c = \sum_{i=1}^{N} P_i R_i\ ; F_c(z^{-1}) = \sum_{k=1}^{N} P_k F_k(z^{-1})\ ; H_c(z^{-1}) = \sum_{k=1}^{N} P_k H_k(z^{-1})\ ;$$

$$\bar{\bar{M}}_c(z^{-1}) = \sum_{k=1}^{N} P_k \bar{\bar{M}}_k(z^{-1})\ ; E_c(z^{-1}) = \sum_{k=1}^{N} P_k[E_k(z^{-1}) + K_k(z^{-1})]\ ;$$

$$\begin{aligned}Q_c(z^{-1}) = {} & P_1' \times diag[q_1^1 \quad q_1^2]_{2\times 2} + P_1' \times diag[q_2^1 z^{-1} \ ....q_2^2 z^{-1}]_{2\times 2} \\ & + ...P_1' \times diag[q_m^1 z^{-m_1+1} \quad q_m^2 z^{-m_2+1}]_{2\times 2}\end{aligned}$$

Eq. (40) can be written as:

$$\begin{aligned}u(k) = {} & R_c w(k) - F_c(z^{-1})y(k) - H_c(z^{-1})u(k-1) \\ & - \bar{\bar{M}}_c(z^{-1})u(k-1) - Q_c(z^{-1})u(k-1) - E_c(z^{-1})v(k)\end{aligned} \quad (41)$$

where $H_c(z^{-1}), Q_c(z^{-1})$ are diagonal polynomial matrices. Define $I + H_c(z^{-1}) + Q_c(z^{-1}) = \bar{H}_c(z^{-1})$, and Eq. (41) can be given by:

$$\bar{H}_c(z^{-1})u(k) = R_c w(k) - F_c(z^{-1})y(k) - \bar{\bar{M}}_c(z^{-1})u(k-1) - E_c(z^{-1})v(k) \quad (42)$$

We define $F_c(z^{-1}) = \sum_{k=1}^{N} P_k F_k(z^{-1}) = \sum_{k=1}^{N} P_k(F_0^j + F_1^j z^{-1} + F_2^j z^{-2})$.

From (42) and (26), we can easily derive K_I, $\bar{\bar{H}}(z^{-1})$, $L(z^{-1})$ $\bar{K}(z^{-1})$. The closed-loop system can be described by:

$$\{z^{-1}F_c(z^{-1})B(z^{-1})+A(z^{-1})[\bar{H}_c(z^{-1})+z^{-1}\bar{\bar{M}}_c(z^{-1})]\}u(k) = R_cA(z^{-1})w(k)-[A(z^{-1})E_c(z^{-1})+z^{-1}F_c(z^{-1})]v(k) \quad (43)$$

In order to guarantee the stability of the closed-loop system, $F_c(z^{-1})$, $\bar{\bar{M}}_c(z^{-1})$ should satisfy:

$$\det\{z^{-1}F_c(z^{-1})B(z^{-1})+A(z^{-1})[\bar{H}_c(z^{-1})+z^{-1}\bar{\bar{M}}_c(z^{-1})]\}\neq 0, |z|\geq 1 \quad (44)$$

C. Adaptive Decoupling Control Based on Neural Networks and Multiple Models

According to (25), the identification equation of system parameters is:

$$y(k)=\Theta^T X(k-1)+v(k-1) \quad (45)$$

where $\Theta=[A_1,\cdots,A_{n_a},B_0,\cdots,B_{n_b}]^T$, $X(k-1)=[-y^T(t-1),\cdots,-y^T(t-n_a),u^T(t-1),\cdots,u^T(t-n_b-1)]^T$.

In this paper, two estimation models are used to predict output of the system. The first one is the linear estimation model :

$$\hat{y}_1(k)=\hat{\Theta}_1^T(k-1)X(k-1) \quad (46)$$

where $\hat{\Theta}_1^T(k-1)$ is an estimation of Θ at instant k–1. The parameter matrix Θ is identified by the following algorithm:

$$\hat{\Theta}_1(k)=\hat{\Theta}_1(k-1)+\frac{\mu_1(k)X(k-1)e_1^T(k)}{1+X(k-1)^TX(k-1)} \quad (47)$$

$$\mu_1(k)=\begin{cases}1 & \text{if } \|e_1(k)\|>4\Delta\\ 0 & \text{else}\end{cases} \quad (48)$$

$e_1(k)$ is the linear model error, i.e.

$$e_1(k)=y(k)-\hat{y}_1(k)=y(k)-\hat{\Theta}_1^T(k-1)X(k-1) \quad (49)$$

The second one is the neural network nonlinear estimation model:

$$\hat{y}_2(k)=\hat{\Theta}_2^T(k-1)X(k-1)+\hat{v}(k-1) \quad (50)$$

where $\hat{v}(k-1)$ can be estimated by multi-layer neural networks[18] and $\hat{\Theta}_2^T(k-1)$ is an another estimation of Θ at instant k–1. The parameter matrix Θ is identified by the following algorithm:

$$\hat{\Theta}_2(k)=\hat{\Theta}_2(k-1)+\frac{\mu_2(k)X(k-1)e_2^T(k)}{1+X(k-1)^TX(k-1)} \quad (51)$$

$$\mu_2(k)=\begin{cases}1 & \text{if } \|e_2(k)\|>4\Delta\\ 0 & \text{else}\end{cases} \quad (52)$$

$e_2(k)$ is the nonlinear model error, i.e.

$$e_2(k)=y(k)-\hat{y}_2(k)=y(k)-\hat{\Theta}_2^T(k-1)X(k-1)-\hat{v}(k-1) \quad (53)$$

If nonlinear item $\hat{v}(k-1)$ is not considered, the linear adaptive decoupling control law based on the linear estimation model is obtained as:

$$\hat{\bar{H}}_1(z^{-1})u(k)=\hat{K}_{I1}w(k)-\hat{L}_1(z^{-1})y(k)-\hat{\bar{\bar{H}}}_1(z^{-1})u(k-1) \quad (54)$$

From (26) and (50), the nonlinear adaptive decoupling control law based on the neural network nonlinear estimation model is obtained as:

$$\hat{\bar{H}}_2(z^{-1})u(k)=\hat{K}_{I2}w(k)-\hat{L}_2(z^{-1})y(k)-\hat{\bar{\bar{H}}}_2(z^{-1})u(k-1)-\hat{\bar{K}}(z^{-1})\hat{v}(k) \quad (55)$$

The linear adaptive decoupling controller (54) can guarantee the stability of the close-loop system. However, it does not consider effects of the nonlinearities on the system output. The performance of control system becomes poor when $\hat{v}(t-1)$ is larger. The nonlinear adaptive decoupling controller (55) can reduce the impact of nonlinearity on system output. But it can not guarantee the stability of the close-loop system. In order to improve performance of control system and ensure the stability for the closed-loop system, a multi- model switching mechanism is obtained [15]:

$$J_i(k)=\sum_{l=1}^{t}\frac{\mu_i(l)(\|e_i(l)\|^2-16\Delta^2)}{4(1+X(l-1)^TX(l-1))}+\alpha\sum_{l=t-N+1}^{t}(1-\mu_i(l))\|e_i(l)\|^2 \quad (i=1,2) \quad (56)$$

$$\mu_i(k)=\begin{cases}1 & \text{if}\|e_i(k)\|>4\Delta\\ 0 & \text{else}\end{cases} \quad (57)$$

where N is an integer and $\alpha\geq 0$ is a predefined constant. $i=1$ stands for the linear model, $i=2$ denotes the nonlinear models. At each time instant t, the linear estimation model and the nonlinear model predict the system output, and the parameters of models are updated through the input-output data. At the same time, we calculate $J_1(k)$, $J_2(k)$ and choose the control law $u^*(k)$ corresponding to the smaller $J^*(k)$ to be applied to the system.

V. Simulation Results

The model parameters and the operating point of the forced circulation as follows:

$Q_F=80m^3/h, \rho_F=1365kg/m^3, x_1=2m, x_2=1429.4kg/m^3,$
$x_3=107.5°c, \rho_w=1365kg/m^3, \lambda_V=2247kJ/kg, A=40m^2$
$\lambda_S=2185kJ/kg, u_1=68m^3/h, u_2=11.2t/h$

In this section, two illustrative examples are provided to demonstrate the performance of the proposed nonlinear decoupling adaptive control. The examples will show the following two scenarios: effect of setpoint changes, parametric uncertainties.

1) In order to study the tracking performance of the multiple models adaptive decoupling controller, the level setpoint does not change during the experiment process. At t=0, product density is changed from $1429.4kg/m^3$ to $1435kg/m^3$, and at t=2h, product density is changed from $1435kg/m^3$ to $1440kg/m^3$,at t=4h, product density is changed from $1440kg/m^3$ to $1435kg/m^3$. For comparison, the conventional cascade PID control strategy is adopted.

2) The changes of the specific heat of the liquor are usually caused by the changes of feed flow. Such changes are usually slow and can not be acquired online. The proposed controller is implemented in a more challenging situation: with a step change from $3.61\ kJ/(kg\cdot{}^0C)$ to $3.63\ kJ/(kg\cdot{}^0C)$, at t=3h. The setpoint of level does not change in this case, and product density is changed from $1429.4kg/m^3$ to $1435kg/m^3$ at t=0. The NMPC (Nonlinear model predictive control) strategy is adopted for comparison.

The system order are $n_a = 2$, $n_b = 1$. We chose $\lambda = I$, N=3, Q_0=diag{0.01 0.03 1 1 1 1}, the parameters of the switching criterion are chosen to be $\alpha = 1$, $N = 2$ and $\Delta = 0.3$. Two groups of multi-layer neural networks are adopted.

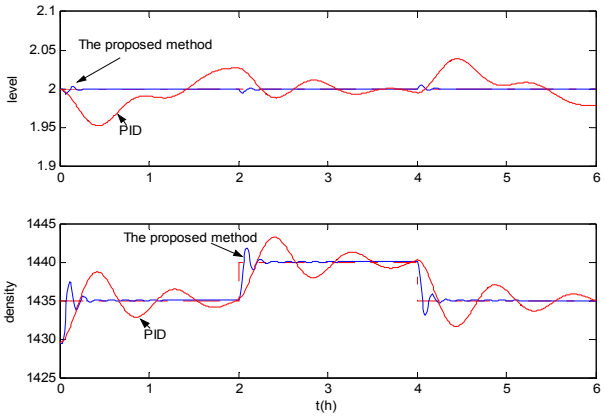

Fig.2 Response of level and product density

The simulation results are shown in Figs.2-3. Fig.2-3 shows the responses of the level and the product density for the conventional cascade strategy, multiple models neural-network-based adaptive decoupling strategy and NMPC strategy.

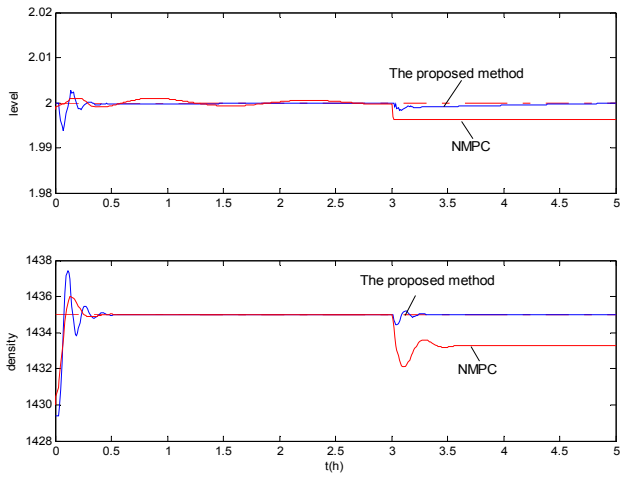

Fig.3 Response of level and product density

It can be seen that the system performance is not good for the conventional cascade PID strategy. The nonlinear multiple models adaptive decoupling can reduce the coupling between the level loop and the density loop. The level of the evaporator is less fluctuations and the product density can track the setpoint quickly. It is worth noting that the proposed method can reduce the uncertainties impact on the system. The level and the density can quickly return the setpoint when the disturbance occurs and the uncertainties parameters change. At the same time, the NMPC strategy applies the forced-circulation system. Although the NMPC can track the setpoint very quickly, it can not reduce the impact of the uncertainties of parameters.

VI. CONCLUSION

The nonlinear multi-model adaptive decoupling control strategy has been proposed in the paper for the forced-circulation system of the alumina production which is a multivariable, strongly coupled nonlinear system with uncertainties. The proposed method can not only mitigate nonlinearities and reduce interactions between the density control and the level control loops, but also improve the transient performance and the evaporation efficiency for the forced-circulation system.

REFERENCES

[1] L.C. To, M.O.Tade. Implementation of a differential geometric nonlinear controller on an industrial evaporator system. *Control Engineering Practice*, Vol.6, no.11, 1309-1319, 1998.

[2] L. C. To, M. O. Tadé, M. Kraetzl, G. P. Le Page. Nonlinear control of a simulated industrial evaporation process. *Journal of Process Control*, vol.5, No.3, 173-182, 1995.

[3] K.M. Kam, M.O.Tade. Simulated Nonlinear control studies of five-effect evaporator models. *Computer and Chemical engineering*, Vol.23, no.11-12, 1795-1810, 2000.

[4] P. Quaak, M. P. C. M. van Wijck, & J. J. Van Haren. Comparison of process identification and physical modelling for falling-film evaporators. *Food Control*, Vol.5, no.2, 73 - 82, 1994.

[5] S. T. Lahtinen. Identification of fuzzy controller for use with a falling-film evaporator. *Food Control*, Vol.12, no.3, 179 - 180, 2001.

[6] J. E. Lozano, M. P. Elustondo, & J. A. Romagnoli. Control studies in an industrial apple juice evaporator. *Journal of food science*, Vol.49, 1422-1427，1984.

[7] G.P. Rangaiah. Nonlinear model predictive control of an industrial four-stage evaporator system via simnlation. *Chemical Engineering journal*, Vol.87, no.3, 285-299, 2002.

[8] P. E. McDermott, D. A. Mellichamp. A decoupling pole placement self-tuning controller for a class of multivariable process [J]. *Optimal Control Applications and Methods*, Vol.7, no.1, 55-79, 1986.

[9] S. J. Lang, X. Y. Gu and T. Y. Chai. A multivariable generalized self-tuning controller with decoupling design. *IEEE Trans. on Automatic Control*, Vol31, no.5, 474-477, 1986.

[10] T. Y. Chai. Direct adaptive decoupling control for general stochastic multivariable systems. International. Journal of Process Control, Vol.51, no.4, 885-909, 1990.

[11] T.P. Zhang; S.S. Ge.. Adaptive Neural Network Tracking Control of MIMO Nonlinear Systems with Unknown Dead Zones and Control Directions. *IEEE Transactions on neural network*, vol.20, no.3, 483-497, 2009.

[12] B. Chaudhuri, R. Majumder, B.C. Pal. Application of multiple-model adaptive control strategy for robust damping of interarea oscillations in power system. *IEEE Transactions on Control Systems Technology*, Vol.12, no.5, 727-736, 2004.

[13] N. V. Q. Hung, H. D. Tuan, T. Narikiyo and P. Apkarian. Adaptive Control for Nonlinearly Parameterized Uncertainties in Robot Manipulators. *IEEE Transactions on Control Systems Technology*, Vol.16, no.3, 458-468, 2008.

[14] K.P. Tee, S.S. Ge, F.E.H. Tay. Adaptive Neural Network Control for Helicopters in Vertical Flight. *IEEE Transactions on Control Systems Technology*, vol.16, no.4, 753-762, 2008.

[15] Y. Fu, T.Y. Chai; Intelligent Decoupling Control of Nonlinear Multivariable Systems and its Application to a Wind Tunnel System. *IEEE Transactions on, Control systems technology*, vol. 17, no. 6, 1376-1384, 2009.